

# Single-Photon-Subtracted-Squeezed-Vacuum-State Based Postselected Weak Measurement and its Applications

Janarbek Yuanbek<sup>1</sup>Akbar Islam<sup>1</sup> Ahmad Abliz<sup>1\*</sup> and Yusuf Turek<sup>2†</sup>

<sup>1</sup>*School of Physics and Electronic Engineering, Xinjiang Normal University, Urumqi, Xinjiang 830054, China and*

<sup>2</sup>*School of Physics, Liaoning University, Shenyang, Liaoning 110036, China*

(Dated: April 30, 2024)

In this paper, we study the effects of postselected von Neumann measurement on the nonclassicality of the Single-Photon-Subtracted-Squeezed-Vacuum-State (SPSSVS). We calculate the squeezing effect, Mandel factor, Wigner function, signal-to-noise ratio (SNR)s and state distance function. We found that postselected von Neumann measurement has positive effects on the optimization of SPSSVS. In particular, by properly choosing the anomalous weak value, the nonclassical inherent features of SPSSVS such as squeezing, photon statistics and phase space distribution can be optimized significantly. The advantages of postselected weak measurement on improving the SNR compared to non-postselected measurement scheme is also confirmed. The superiority of SPSSVS based postselected weak measurement in quantum state optimization may have potential applications of in the associated quantum information processing.

## I. INTRODUCTION

As is well known, the information of a microscopic system is contained in its quantum state. Therefore, it is of utmost importance to find the quantum state that describes a microscopic system. While any quantum system can be described by its corresponding quantum state, not all states exhibit good nonclassical properties. The quantum weak measurements proposed by physicists such as Aharonov, Albert, and Vaidman in the late 1980s not only generalize the original measurement theory but also provide a good solution for the development of quantum control [1]. In a single weak measurement, the information obtained from the measured system by the measuring instrument is limited. Nevertheless, the partially collapsed quantum state can still retain some information through repetitive measurements, thereby significantly increasing the measurement accuracy. Using the weak signal amplifying principle, the weak measurement method also amplifies measurement results with large values, even in the weak coupling regime. In quantum optics, photon number statistics are used to describe the nonclassical properties of radiated light fields. A significant amount of theoretical and experimental work has been conducted in this area to confirm the effectiveness of squeezing effects and phase-space distribution functions. The preparation and optimisation of non-classical properties of the quantum state are vital in quantum information processing, including the generation and detection of single photons [2, 3], quantum computing [4, 5], quantum teleportation [6–12], generation and manipulation of atom-light entanglement and precision measurements [13]. However, the realisation of these processes depends on the generating, analysing and optimisation of the relevant quantum states, such as

the coherent state [14–16], squeezing state [17–19], photon number states [20–26], even and odd coherent states [27, 28]. However, with the emerge of state-of-the-art technologies, the above mentioned states can no longer meet the needs of practical applications in quantum information science. The construction of new quantum states has become a new pursuit for researchers in related fields. In recent years, various schemes have been proposed for creating new quantum states and their related properties have been investigated to some extent[29].

In this manuscript, we study the application of post-selective measurement theory to precision measurements using the SPSSVS [30, 31] as a pointer. In order to investigate the advantages of the SPSSVS-based post-selective weak measurements in precision measurements, we present both the analytical expressions and numerical results including the second-order correlation function, Mandel factor, squeezing effect, Wigner function, SNR and state distance. The results show that the SPSSVS exhibits weaker statistical properties of the sub-Poisson photon distribution. Theoretical analyses show that the post-selective measurement theory with the SPSSVS as a pointer state does have weaker nonclassical properties than the original state [32].

This paper is organized as follows. In Sec. II A, we introduce the main concepts of our scheme and the final pointer state after the postselected measurement, which will be used throughout the study, then we give details of the squeezing effects of the final pointer state by using the definition of squeezing. In the subsequent sections, we study Mandel factor and Wigner function of the SPSSVS. In Sec. III we calculate the SNR of SPSSVS after postselected measurement. In Sec. IV state distance is analyzed in order to examine the effects of postselected measurement on the initial state. In Sec. V we present our conclusion and remarks.

\* aahmad@126.com

† yusuftu1984@hotmail.com

## II. THE EFFECTS OF POSTSELECTED MEASUREMENT ON THE PROPERTIES OF SPSSVS

In measurement theory, the total Hamiltonian has a general form of consisting three parts as  $\hat{H} = \hat{H}_s + \hat{H}_p + \hat{H}_{int}$ . Here,  $\hat{H}_s$  and  $\hat{H}_p$  represent the Hamiltonians of the measured system and pointer (measuring device), respectively, and  $\hat{H}_{int}$  is the interaction Hamiltonian. According to the ideal measurement theory [33], the explicit expressions of the Hamiltonian for the pointer and measured system do not affect the measurement results. This interaction Hamiltonian contains the main information about the pointer and the measured system. In this work we take the interaction Hamiltonian as

$$\hat{H}_{int} = g\delta(t - t_0)\hat{\sigma}_x \otimes \hat{P}. \quad (1)$$

The function  $g\delta(t - t_0)$  represents the interaction coupling between the pointer and the measured system, and  $\int_0^t g\delta(t - t_0)d\tau = g$ .  $\hat{\sigma}_x = |\uparrow_x\rangle\langle\uparrow_x| - |\downarrow_x\rangle\langle\downarrow_x|$  is the Pauli  $x$  operator of the system to be measured and  $|\uparrow_x\rangle$  and  $|\downarrow_x\rangle$  are the eigenstates of  $\hat{\sigma}_x$  with corresponding eigenvalues 1 and  $-1$ , respectively. In the above Hamiltonian the  $\hat{P}$  denotes the momentum operator of the pointer which is the conjugate of  $\hat{X}$  and  $[\hat{X}, \hat{P}] = i\hat{I}$ . Our goal in this work is to investigate the effects of post-selected measurement on the inherent properties of the SPSSVS. Thus, in the present work, we take the polarization and spatial degrees of freedom of the SPSSVS as the measured system and pointer, respectively. We assume that the initial state of the total system is prepared as  $|\psi_i\rangle \otimes |\phi\rangle$ . Here  $|\psi_i\rangle = \cos\frac{\alpha}{2}|\uparrow_z\rangle + e^{i\delta}\sin\frac{\alpha}{2}|\downarrow_z\rangle$  with  $\delta \in [0, 2\pi]$  and  $\alpha \in [0, \pi)$ ,  $|\phi\rangle$  is the SPSSVS defined as

$$|\phi\rangle = \kappa\hat{a}|\xi\rangle = \kappa\hat{a}\hat{S}(\xi)|0\rangle. \quad (2)$$

Here,  $\kappa = \sinh^{-1} r$  and  $\hat{S}(\xi) = \exp[\frac{1}{2}\xi\hat{a}^{\dagger 2} - \frac{1}{2}\xi^*\hat{a}^2]$ ,  $\xi = re^{i\theta}$  is the squeezing operator. The initial state  $|\psi_i\rangle$  can be prepared in the optical lab by using quarter and half wave plates. Under the unitary evolution operator  $\hat{U}(t) = \exp\left(-i\int_0^t \hat{H}_{int}d\tau\right)$ , the state  $|\psi_i\rangle \otimes |\phi\rangle$  evolves to

$$\begin{aligned} |\Psi\rangle &= e^{-ig\hat{\sigma}_x \otimes \hat{P}_x} |\psi_i\rangle \otimes |\phi\rangle \\ &= \frac{1}{2} \left[ (\hat{I} + \hat{\sigma}_x) \otimes \hat{D}\left(\frac{s}{2}\right) + (\hat{I} - \hat{\sigma}_x) \otimes \hat{D}\left(-\frac{s}{2}\right) \right] |\psi_i\rangle \otimes |\phi\rangle. \end{aligned} \quad (3)$$

In the derivation of the above expression we have written the momentum operator  $\hat{P}$  in terms of the annihilation and creation operator,  $\hat{a}$  and  $\hat{a}^\dagger$ , as  $\hat{P}_x = \frac{i}{2\sigma}(\hat{a}^\dagger - \hat{a})$ , and  $\hat{D}\left(\frac{s}{2}\right) = \exp\left[\frac{s}{2}(\hat{a}^\dagger - \hat{a})\right]$ . The parameter  $s$  is the ratio between the coupling  $g$  and beam width  $\sigma$ , i.e.,  $s = \frac{g}{\sigma}$ . It takes continuous value and could characterize the measurement strength. If  $0 < s < 1$  ( $s > 1$ ), the measurement

is called weak (strong) measurement. For the implementation of the postselected von Neumann measurement, the state  $|\psi_f\rangle = |\uparrow_z\rangle$  is taken as the postselecting state onto the Eq.(3), then the normalized final state of the pointer can be obtained as

$$|\Phi\rangle = \lambda \left[ (1 + \langle\hat{\sigma}_x\rangle_w) \hat{D}\left(\frac{s}{2}\right) + (1 - \langle\hat{\sigma}_x\rangle_w) \hat{D}\left(-\frac{s}{2}\right) \right] |\phi\rangle, \quad (4)$$

where the normalization coefficient  $\lambda$  is defined as

$$\lambda = \frac{1}{\sqrt{2}} [1 + |\langle\hat{\sigma}_x\rangle_w|^2 + (1 - |\langle\hat{\sigma}_x\rangle_w|^2)(1 - |\beta|^2)e^{-\frac{1}{2}|\beta|^2}]^{-\frac{1}{2}}$$

with  $\beta = -s[\cosh(r) - e^{i\theta}\sinh(r)]$ . As the result of postselected measurement, the weak value of system observable  $\hat{\sigma}_x$  is given by

$$\langle\hat{\sigma}_x\rangle_w = \frac{\langle\psi_f|\hat{\sigma}_x|\psi_i\rangle}{\langle\psi_f|\psi_i\rangle} = e^{i\delta} \tan\frac{\alpha}{2}. \quad (5)$$

The Eq.(4) is the final state of the pointer after postselected von Neumann measurement, which will be used throughout our work. It can be easily seen that the weak value above can go beyond the scope of the normal values of observable  $\sigma_x$  and even takes a complex value if the case of  $\delta \neq 0$  is taken into account. As mentioned in the introduction part, the anomalous large weak values can not only be used to amplify the tiny system information and also be used to optimize the quantum states. Next we examine the effects of anomalous values of measured system observable on the inherent properties of SPSSVS.

### A. Squeezing parameter

In this subsection, we study the effects of postselected von Nuemann measurement on the squeezing parameter of SPSSVS. Squeezing effects plays a crucial role in quantum theory and its applications. Squeezing refers to the case where the quantum fluctuation in a state is less than the vacuum fluctuation. Thus, the states with squeezing effects are considered to be genuine non-classical states [34], and there is no classical counterpart [35, 36] of them. Research on squeezing effects, especially on orthogonal squeezing effects, has been conducted in optical communications and information theory [12, 37–41], gravitational wave detection [6], intensive encoding [42], resonance fluorescence [43] and quantum cryptography [44] etc.

The squeezing parameter of a radiation field is defined as

$$\hat{S}_\phi = (\Delta\hat{X}_\phi)^2 - \frac{1}{2}, \quad (6)$$

where

$$\hat{X}_\phi = \frac{1}{\sqrt{2}}(\hat{a}e^{-i\phi} + \hat{a}^\dagger e^{i\phi}). \quad (7)$$

is a quadrature operator of the field and satisfies  $[\hat{X}_\phi, \hat{X}_{\phi+\frac{\pi}{2}}] = i$ ,  $\phi = 0, \frac{\pi}{2}$ . The variance of  $\hat{X}_\phi$  is defined as  $(\Delta\hat{X}_\phi)^2 = \langle \Phi | \hat{X}_\phi^2 | \Phi \rangle - \langle \Phi | \hat{X}_\phi | \Phi \rangle^2$  under the state  $|\Phi\rangle$ . From the definition of  $\hat{S}_\phi$ , it can be seen that  $\hat{S}_\phi \geq -\frac{1}{2}$ . If  $-\frac{1}{2} \leq \hat{S}_\phi \leq 0$ , then there occurs squeezing effect of corresponding radiation field in phase space along  $\phi = 0$  or  $\frac{\pi}{2}$  direction. Next we calculate the above quantities under the state  $|\Phi\rangle$  which is given in Eq.(4). By a straightforward calculation we can get that

$$\langle \hat{X}_\phi \rangle = \frac{1}{\sqrt{2}} \langle \hat{a}e^{-i\phi} + \hat{a}^\dagger e^{i\phi} \rangle = \sqrt{2} \Re [\langle \hat{a} \rangle e^{-i\phi}] \quad (8)$$

and

$$\begin{aligned} \langle \hat{X}_\phi^2 \rangle &= \frac{1}{2} \langle (\hat{a}e^{-i\phi} + \hat{a}^\dagger e^{i\phi})(\hat{a}e^{-i\phi} + \hat{a}^\dagger e^{i\phi}) \rangle \\ &= \Re [\langle \hat{a}^2 \rangle e^{-2i\phi}] + \langle \hat{a}^\dagger \hat{a} \rangle + \frac{1}{2}. \end{aligned} \quad (9)$$

The explicit expressions of  $\langle \hat{X}_\phi \rangle$  and  $\langle \hat{X}_\phi^2 \rangle$  can be obtained by calculating the expectation values of  $\langle \hat{a} \rangle, \langle \hat{a}^2 \rangle$  and  $\langle \hat{a}^\dagger \hat{a} \rangle$  under the state  $|\Phi\rangle$  which are given as

$$\langle \hat{a} \rangle = |\lambda|^2 [2\Re[\langle \hat{\sigma}_x \rangle_w] s - 2i\Im[\langle \hat{\sigma}_x \rangle_w] h_1(s)], \quad (10)$$

$$\begin{aligned} \langle \hat{a}^2 \rangle &= |\lambda|^2 [(1 + |\langle \hat{\sigma}_x \rangle_w|^2)(3e^{i\theta} \sinh(2r) + \frac{s^2}{2}), \\ &+ 2(1 - |\langle \hat{\sigma}_x \rangle_w|^2) h_2(s)], \end{aligned} \quad (11)$$

and

$$\begin{aligned} \langle \hat{a}^\dagger \hat{a} \rangle &= 2|\lambda|^2 [(1 + |\langle \hat{\sigma}_x \rangle_w|^2)(1 + 3\sinh^2(r) + \frac{s^2}{4}) \\ &+ (1 - |\langle \hat{\sigma}_x \rangle_w|^2) h_3(s)], \end{aligned} \quad (12)$$

respectively. Here,

$$\begin{aligned} h_1(s) &= [\beta \cosh(r)(\beta^2 e^{-i\theta} \coth(r) + 3) \\ &+ \frac{s}{2}(2\beta^2 e^{-i\theta} \coth(r) - |\beta|^2 + 3)] e^{-\frac{1}{2}|\beta|^2}, \end{aligned} \quad (13)$$

$$\begin{aligned} h_2(s) &= \{\beta^2 \cosh^2(r)[\beta^2 e^{-i\theta} \coth(r) + 6] + \frac{3}{2} e^{i\theta} \sinh(2r) \\ &- 2s\beta \cosh(r)(\beta^2 e^{-i\theta} \coth(r) + 3) \\ &+ \frac{s^2}{4}[2\beta^2 e^{-i\theta} \coth(r) - |\beta|^2 + 3]\} e^{-\frac{1}{2}|\beta|^2}, \end{aligned} \quad (14)$$

and

$$\begin{aligned} h_3(s) &= \{\beta^2 e^{-i\theta} [\coth(r) \cosh^2(r) + 5 \sinh(r) \cosh(r) \\ &+ \beta^2 e^{-i\theta} \cosh^2(r)] + 1 + 3 \sinh^2(r) \\ &+ \frac{3s}{2} \beta e^{-i\theta} [\frac{1 + 3 \sinh^2(r)}{\sinh(r)} + \beta^2 e^{-i\theta} \cosh(r)] \\ &+ \frac{s^2}{2} e^{-i\theta} [\coth(r) + \beta^2 e^{-i\theta}] + \frac{se^{-i\theta}}{2} \beta^3 \cosh(r) \coth(r) \\ &+ \frac{3s}{2} \beta \cosh(r) + \frac{s^2}{4} [2\beta^2 e^{-i\theta} \coth(r) - |\beta|^2 + 3]\} e^{-\frac{1}{2}|\beta|^2}. \end{aligned} \quad (15)$$

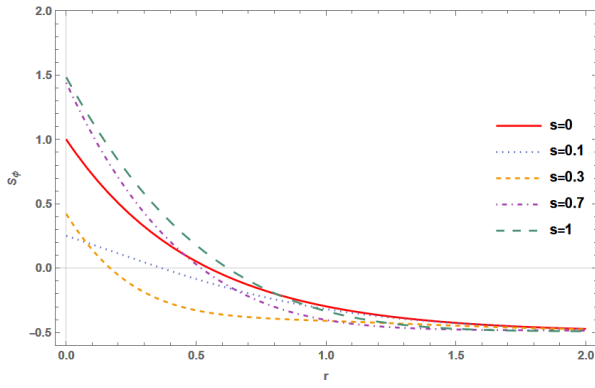
By substituting the above expressions into Eq. (6) we can obtain the squeezing parameter of SPSSVS under the state  $|\Phi\rangle$ . Since its explicit expression is too cumbersome to analytically analyze, we give numerical results. The numerical results for different parameters are shown in Fig.1. In Fig.1a, we presented the  $\hat{S}_{\pi/2}$  as a function of squeezing parameter  $r$  for different coupling strength  $s$  while the weak value is fixed to  $\langle \hat{\sigma}_x \rangle_w = 5.76$  ( $\alpha = 8\pi/9$ ). As we can see in the weak measurement regime ( $0 < s \ll 1$ ), the squeezing parameter  $\hat{S}_{\pi/2}$  takes lower values than the initial state  $|\phi\rangle$ . In Fig.1b the dependence of  $\hat{S}_{\pi/2}$  on the coupling strength  $s$  for different anomalous weak values and fixed squeezing parameter  $r=0.5$ . The larger the anomalous weak values, the larger the squeezing parameters. The squeezing parameter  $\hat{S}_{\pi/2}$  as a function of anomalous weak values is plotted in Fig.1c for different  $s$ . All these results further confirm that the squeezing effect of SPSSVS is increased after taking weak measurement.

## B. Mandel factor

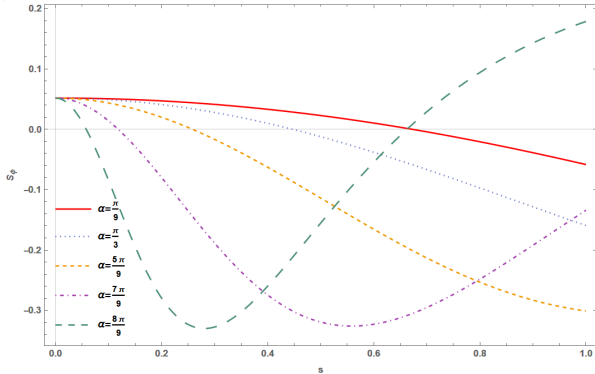
The photon number statistics of a radiant light field typically exhibit three types of distributions: super-Poissonian, Poisson, and sub-Poissonian. The Poisson distribution is the statistical distribution of a beam of perfectly coherent light with constant intensity, and serves as a benchmark for classifying statistical distributions. A distribution that is broader than the Poisson distribution is referred to as a super-Poissonian distribution, while a distribution that is narrower than the Poisson distribution is referred to as a sub-Poissonian distribution. The sub-Poissonian distribution exhibits lower photon number fluctuations compared to the Poisson distribution, and lacks a classical counterpart. Therefore, it is important to describe the state using non-classical terminology with and mandel factor. In this subsection, we investigate the Mandel factor  $Q_m$  for the  $|\Phi\rangle$  state.

The mathematical definition of the Mandel factor  $Q_m$  of a single-mode radiation field is given as

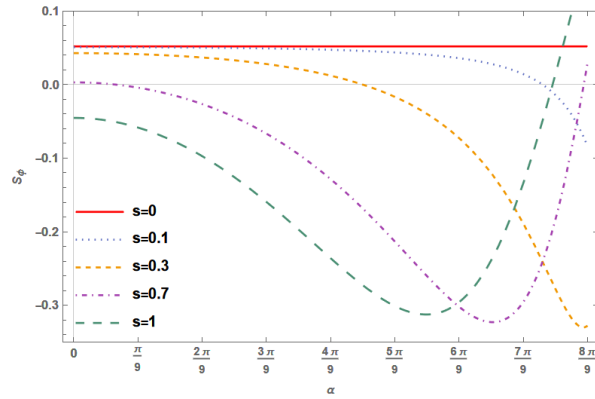
$$Q_m = \frac{\langle \hat{a}^{\dagger 2} \hat{a}^2 \rangle}{\langle \hat{a}^\dagger \hat{a} \rangle} - \langle \hat{a}^\dagger \hat{a} \rangle. \quad (16)$$



(a)



(b)



(c)

Figure 1: Squeezing Parameter of SPSSVS under  $|\Phi\rangle$  for different system parameters. (a)  $S_\phi$  as a function of  $r$  for different coupling strength parameter  $s$  while fixed the weak value parameter  $\alpha = \frac{8\pi}{9}$ . (b)  $S_\phi$  as a function of  $s$  for different weak values while fixed squeezing state parameter  $r = 0.5$ . (c)  $S_\phi$  as a function of weak values characterized by  $\alpha$  for different  $s$  while keeping  $r = 0.5$ .

Here, we take  $\theta = 0, \delta = \phi = \frac{\pi}{2}$

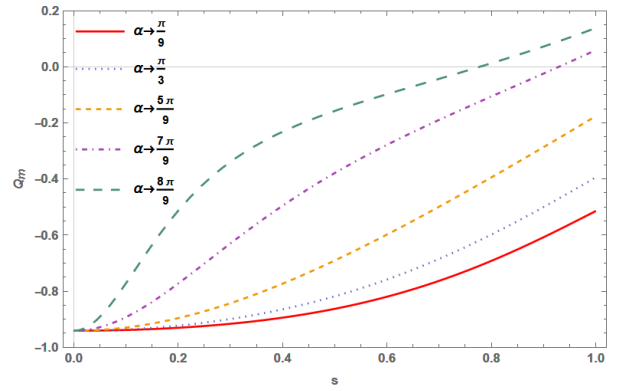


Figure 2: Mandel Factor  $Q_m$  of the SPSSVS after psotselected measurement. Here  $\theta = 0, \delta = \frac{\pi}{2}, r = 0.1$

If  $-1 \leq Q_m < 0$ , the field exhibits sub-Poissonian statistics and is purely non-classical, and the Mandel factor can never be less than  $-1$  for any cases [45].

In Fig.2 the variation of  $Q_m$  with the coupling strength  $s$  is plotted for the fixed value of  $\alpha$ . It is evident that, as the weak value increases, the nonclassical nature weakens.

It is also observed that the nonclassical properties weaken as  $s$  shifts from the weak measurement to the strong one. We noted that for postselected von Neumann measurements based on SPSSVS, the value of  $Q_m$  decreases significantly with very large weak values. This is contrary to the signal amplification feature verified in previous studies[46–48].

### C. Wigner function

In order to deeply understand the effects of postselected von Neumann measurement on the inherent properties of SPSSVS, in this subsection, we examine the phase space distribution of SPSSVS by calculating the Wigner function. Wigner function contains the quasi-probability distribution of the quantum state, phase, and other important information, similar to the wave function or density matrix corresponding to a quantum state. A negative value of Wigner function of a given state means the nonclassicality of that state. The bigger negative region in phase space a state has, the more nonclassicality it has. In order to obtain even more information about the state  $|\Phi\rangle$ , it is necessary to investigate the Wigner function in phase space. In general, the Wigner function is defined as the two-dimensional Fourier transform of the symmetric order eigenfunction. The general expression of Wigner function for a state  $\rho = |\Phi\rangle\langle\Phi|$  is given by [49]

$$W(z) \equiv \frac{1}{\pi^2} \int_{-\infty}^{+\infty} \exp(\lambda^* z - \lambda z^*) C_W(\lambda) d^2 \lambda. \quad (17)$$

where  $C_W(\lambda)$  is the symmetrically ordered characteristic function defined as

$$C_W(\lambda) = \text{Tr} \left[ \rho e^{\lambda \hat{a}^\dagger - \lambda^* \hat{a}} \right]. \quad (18)$$

Here, we use the notation of  $\lambda'$  and  $\lambda''$  for the real and imaginary parts of  $\lambda$  and set  $z = x + ip$  to emphasize the analogy between the quadratic radiation field and the normalized dimensionless position and momentum observables of the beam in phase space. We can rewrite the definition of the Wigner function in terms of  $x, p$  and  $\lambda', \lambda''$  as

$$W(x, p) = \frac{1}{\pi^2} \int e^{2i(p\lambda' - x\lambda'')} C_W(\lambda) d\lambda' d\lambda''. \quad (19)$$

To show the effects of the postselected von Neumann measurement on the non-classical feature of SPSSVS, in Fig.3 we plot the Wigner function of SPSSVS for different squeezing parameters  $r$  and coupling strengths  $s$ . Each column from left to right indicates the different coupling strengths  $s$  for 0, 0.1, 0.5 and 1, and each row from up to down represents the different squeezing parameters  $r$  for 0, 0.5, 1 and 2. Here, we take the weak value as  $\langle \hat{\sigma}_x \rangle_w = 5.76$  ( $\alpha = 8\pi/9$ ). It is observed that as showed in squeezing parameter  $\hat{S}_{\pi/2}$ , there always occur squeezing effects along  $y$ -axis, which are increased in weak measurement regimes. As is shown, the positive peaks of the Wigner function gradually becomes irregular with increasing the coupling strength  $s$ . Furthermore, in Fig.3 for  $s = 0.5, 1$  and  $r = 0.5, 1$  cases we can see that significant interference structures manifest and the negative regions become larger than the initial pointer state.

As mentioned above, the existence of and progressively stronger negative regions of the Wigner function in phase space indicates the degree of nonclassicality of the associated state. From the above analysis we can conclude that after the postselected von Neumann measurement, the phase space distribution of SPSSVS is not only more squeezed but its nonclassicality also gets more obvious in the most regimes.

### III. SIGNAL-TO-NOISE RATIO

In precision measurement it is important to get precise information while suppress the associated noise. To demonstrate the superiority of SPSSVS-based postselected measurement over non-postselected measurement[45] for position shift, the SNR between postselected and non-postselected measurement is ana-

lyzed, which is characterized as below

$$\chi = \frac{\mathcal{R}_p}{\mathcal{R}_n}. \quad (21)$$

where  $\mathcal{R}_p$  represents the SNR of postselected von Neumann measurement which is defined by

$$\mathcal{R}_p = \frac{\sqrt{NP_s} |\delta x|}{\Delta x} \quad (22)$$

with the variance of position operator

$$\Delta x = \sqrt{\langle \Phi | \hat{X}^2 | \Phi \rangle - \langle \Phi | \hat{X} | \Phi \rangle^2}, \quad (23)$$

and the average shift of the pointer variable  $x$  after postselected measurement

$$\delta x = \langle \Phi | \hat{X} | \Phi \rangle - \langle \phi | \hat{X} | \phi \rangle. \quad (24)$$

Here,  $\hat{X} = \sigma(\hat{a} + \hat{a}^\dagger)$  is the position operator,  $N$  is the total number of measurements, and  $P_s = |\langle \psi_f | \psi_i \rangle|^2 = \cos^2 \frac{\alpha}{2}$  is the success probability of postselection, and  $|\Phi\rangle$  denotes the normalized state of SPSSVS after postselection which is given by Eq.(4). We know that

$$\langle \phi | \hat{X} | \phi \rangle = 2\sigma \Re[\langle \phi | \hat{a} | \phi \rangle] \quad (25)$$

$$\langle \Phi | \hat{X} | \Phi \rangle = 2\sigma \Re[\langle \Phi | \hat{a} | \Phi \rangle] \quad (26)$$

$$\langle \Phi | \hat{X}^2 | \Phi \rangle = \sigma^2 (2\langle \Phi | \hat{a}^\dagger \hat{a} | \Phi \rangle + 2\text{Re}[\langle \Phi | \hat{a}^2 | \Phi \rangle] + 1) \quad (27)$$

Furthermore, the SNR  $\mathcal{R}_n$  for non-postselected measurement is defined as

$$\begin{aligned} W(z) &= \frac{1}{\pi^2} \int \int d\lambda d\lambda^* \text{Tr} [\rho D(\lambda)] e^{-(\lambda \alpha^* - \lambda^* \alpha)} \\ &= |\lambda|^2 [1 + \langle \hat{\sigma}_x \rangle_w]^2 \frac{2}{\pi} (4|\alpha' - s\Gamma|^2 - 1) e^{-2|\alpha' - s\Gamma|^2} \\ &\quad + |1 - \langle \hat{\sigma}_x \rangle_w|^2 \frac{2}{\pi} (4|\alpha' + s\Gamma|^2 - 1) e^{-2|\alpha' + s\Gamma|^2} \\ &\quad + \frac{4}{\pi} \Re \left[ (1 + \langle \hat{\sigma}_x \rangle_w) (1 - \langle \hat{\sigma}_x \rangle_w)^* e^{-2s(\alpha - \alpha^*) - 2|\alpha'|^2} \right] \\ &\quad \times (4|\alpha'|^2 - 1), \end{aligned} \quad (20)$$

where  $\Gamma = \cosh(r) - e^{i\theta} \sinh(r)$  and  $\alpha' = \alpha \cosh(r) - \alpha^* e^{i\theta} \sinh(r)$ . In general, this is a real Wigner function and its value is bounded as  $-\frac{2}{\pi} \leq W(z) \leq \frac{2}{\pi}$  in whole phase space.

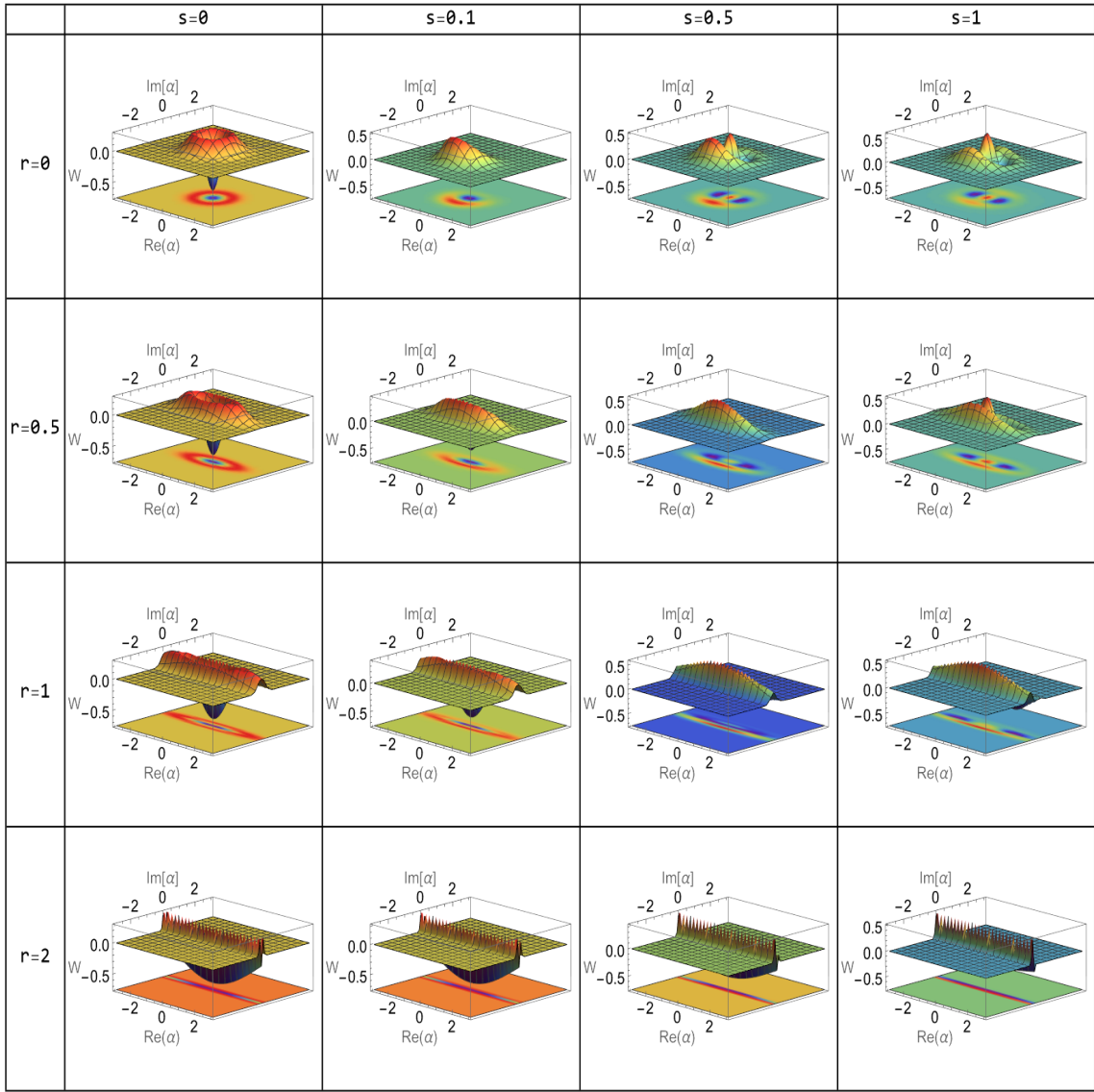


Figure 3: (Color Online) The Wigner function of SPSSVS after postselected von Neumann measurement. Here, we take  $\theta = 0, \delta = \frac{\pi}{2}, \alpha = \frac{8\pi}{9}$ . Each column represents different measurement strengths with  $s=0,0.1,0.5,1$ , and are ordered accordingly from left to right.

$$\mathcal{R}_n = \frac{\sqrt{N}|\delta x'|}{\Delta x'} \quad (28)$$

with

$$\begin{aligned} \Delta x' &= \sqrt{\langle \Psi | \hat{X}^2 | \Psi \rangle - \langle \Psi | \hat{X} | \Psi \rangle^2}, \\ \delta x' &= \langle \Psi | \hat{X} | \Psi \rangle - \langle \phi | \hat{X} | \phi \rangle. \end{aligned} \quad (29)$$

Here, we have to note that  $|\Psi\rangle$  is the normalized final state of the total system without taking postselection as is given in Eq.(3).

The expectation values of  $\langle \hat{a} \rangle$ ,  $\langle \hat{a}^\dagger \hat{a} \rangle$  and  $\langle \hat{a}^2 \rangle$  under the state  $|\Psi\rangle$  are given as

$$\langle \Psi | \hat{a} | \Psi \rangle = \frac{s}{2} \sin \alpha \cos \delta, \quad (30)$$

$$\langle \Psi | \hat{a}^\dagger \hat{a} | \Psi \rangle = 1 + 3 \sinh^2(r) + \frac{s^2}{4}, \quad (31)$$

and

$$\langle \Psi | \hat{a}^2 | \Psi \rangle = \frac{1}{2} (3e^{i\theta} \sinh(2r) + \frac{s^2}{4}), \quad (32)$$

respectively.

In Fig.4, we show the ratio  $\chi$  of SNRs between postselected and nonpostselected von Neumann measurement for different system parameters. As presented in Fig.4a,

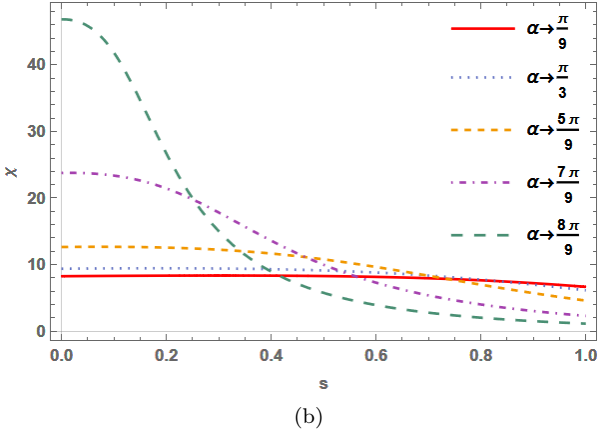
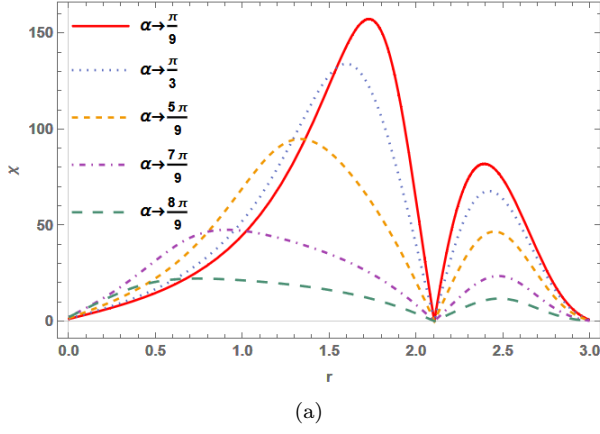


Figure 4: (Color online ) The ratio  $\chi$  of SNRs of SPSSVS between postselected and non-postselected measurement cases . Here, we take  $\theta = \frac{5\pi}{12}, \delta = \frac{\pi}{2}$ , In (a),  $\chi$  is plotted as a function of squeezing parameter  $r$  for different weak values while fixed  $s = 0.3$ . In (b),  $\chi$  is plotted as a function of coupling strength parameter  $s$  for different weak values for the fixed coupling paramter  $r = 0.3$ .

we plot the ratio  $\chi$  as a function of the coherent state parameter  $r$  and we can see that in the weak measurement regime the ratio  $\chi$  of SNRs exhibits a slightly damping periodic oscillation with the increasing of system parameter  $r$ , and in the most of the regions, the ratio  $\chi$  is much larger than one. Furthermore, as indicated in Fig.4b, the ratio  $\chi$  increases in weak measurement regime ( $s \ll 1$ ) for large anomalous weak values. In a word, it can be found that the signal-to-noise ratio of SPSSVS after which is postselected measurement is increased dramatically in weak measurement regime for large weak values compared to nonpostselected measurement case. This result indicates that SPSSVS may have potential applications in the associated precision measurement problems after taking postselected weak measurement procedure.

#### IV. STATE DISTANCE

As discussed in above context, the inherent properties of SPSSVS are changed dramatically after taking postselected von Neumann measurement. As shown in previous studies, the postselected measurement could change the state, and it may also be a reason to change the nonclassical features of original given state. In this section, to examine the effects of postselected measurement on the initial state  $|\phi\rangle$ , we check the state distance. In quantum information theory the distance between two quantum states described by density operators  $\rho$  and  $\sigma$ , is defined as

$$F = \left( \text{Tr} \sqrt{\sqrt{\rho}\sigma\sqrt{\rho}} \right)^2. \quad (33)$$

This formula also can characterize the fidelity (and is also called Uhlmann-Jozsa fidelity) between two states. In our present study both states are pure i.e.,  $\rho = |\phi\rangle\langle\phi|$  and  $\sigma = |\Phi\rangle\langle\Phi|$ , then the above formula can be rewritten as

$$F = |\langle\phi|\Phi\rangle|^2. \quad (34)$$

Its value is bounded  $0 \leq F \leq 1$ . If  $F = 1$  ( $F = 0$ ), then the two states are exactly the same (totally different). This quantity is a natural candidate for the state distance because it corresponds to the closeness of states in the Hilbert space. The inner product of  $|\phi\rangle$  and  $|\Phi\rangle$  is calculated as

$$\langle\phi|\Phi\rangle = \lambda [(1 + \langle\hat{\sigma}_x\rangle)P_1(s) + (1 - \langle\hat{\sigma}_x\rangle)P_2(s)], \quad (35)$$

where

$$P_1(s) = [\beta^2 e^{-i\theta} \coth(r) + 1] e^{-\frac{1}{2}|\beta|^2} - \frac{s\beta e^{-i\theta}}{2 \sinh(r)}, \quad (36)$$

and

$$P_2(s) = [\beta^2 e^{-i\theta} \coth(r) + 1] e^{-\frac{1}{2}|\beta|^2} + \frac{s\beta e^{-i\theta}}{2 \sinh(r)}. \quad (37)$$

In Fig.5, the fidelity  $F$  is plotted as a function of coupling strength  $s$  for the fixed  $r = 0.5$ . As showed in Fig.5, the fidelity between  $|\phi\rangle$  and  $|\Phi\rangle$  is gradually decreased with increasing the coupling strength and weak values. This indicates that the postselected von Neumann measurement can change the inherent properties of initial given state by destroying the given state gradually and change it to another state as some quantum state engineering processes.

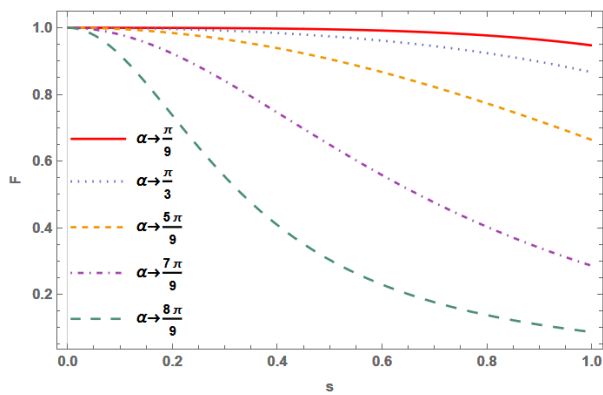


Figure 5: (color online) The state distance between  $|\phi\rangle$  and  $|\Phi\rangle$ . Here we take  $r = 0.5, \theta = 0, \delta = \frac{\pi}{2}$ .

## V. CONCLUSION AND REMARKS

In summary, we investigated the effects of postselected von Neumann measurement on the properties of SPSSVS. We firstly presented both the analytical and numerical results of Mandel factors, squeezing parameter, and Wigner function of final pointer states. It is found that in weak measurement regime the squeezing effect is increased dramatically for anomalous weak values. We also noticed that the postselected measurement has no positive effect to the Mandel factor of SPSSVS. By investigating the Wigner function we found that in weak

measurement regime the negativity of Wigner function of SPSSVS is increased compared to the initial state. These results showed that postselected von Neumann measurement can increase the nonclassicality of SPSSVS in weak measurement regime by properly choosing the anomalous weak values. Furthermore, the comparison of SNRs between postselected and non-postselected measurement cases showed that the SNR of postselected measurement scheme is much larger than non-postselected case. We noticed that in this process the amplification effect of weak value played a significant role although the postselection probability is low in this case.

To conclude, in our current work, we investigated the effects of postselected von-Neumann measurement on the inherent properties of the SPSSVS. However, real light beams are time-dependent, and representing this dependence needs two or more modes of the optical systems. Therefore, it would be interesting to investigate the impact of postselected von-Neumann measurements on other relevant radiation fields, such as pair-coherent state (two-mode radiation field)[28, 50] and other multi-mode radiation fields [51] as well.

## ACKNOWLEDGMENTS

This work was supported by the National Natural Science Foundation of China (No. 12365005) and (No. 11864042).

- 
- [1] Y. Aharonov, D. Z. Albert, and L. Vaidman, *Phys. Rev. Lett.* **60**, 1351 (1988).
  - [2] H. Yonezawa and A. Furusawa, *Opt Spectrosc+* **108**, 288 (2010).
  - [3] Z. Zhang and L. M. Duan, *New. J. Phys* **16**, 103037 (2014).
  - [4] A. Blais, S. M. Girvin, and W. D. Oliver, *Nat. Phys* **16**, 247 (2020).
  - [5] M. A. Nielsen and I. L. Chuang, *Quantum Computation and Quantum Information* (Cambridge University Press, Cambridge, England, 2010).
  - [6] B. Schumacher, *Phys. Rev. A* **54**, 2614 (1996).
  - [7] B. Schumacher and M. A. Nielsen, *Phys. Rev. A* **54**, 2629 (1996).
  - [8] G. J. Milburn and S. L. Braunstein, *Phys. Rev. A* **60**, 937 (1999).
  - [9] T. C. Zhang, K. W. Goh, C. W. Chou, P. Lodahl, and H. J. Kimble, *Phys. Rev. A* **67**, 033802 (2003).
  - [10] B. Kraus, K. Hammerer, G. Giedke, and J. I. Cirac, *Phys. Rev. A* **67**, 042314 (2003).
  - [11] A. Dolińska, B. C. Buchler, W. P. Bowen, T. C. Ralph, and P. K. Lam, *Phys. Rev. A* **68**, 052308 (2003).
  - [12] C. M. Caves, *Phys. Rev. D* **23**, 1693 (1981).
  - [13] B. Hacker, S. Welte, S. Daiss, A. Shaikat, S. Ritter, L. Li, and G. Rempe, *Nature Photonics* **13**, 110 (2018).
  - [14] R. J. Glauber, *Phys. Rev.* **131**, 2766 (1963).
  - [15] U. M. Titulaer and R. J. Glauber, *Phys. Rev.* **140**, B676 (1965).
  - [16] D. Stoler, *Phys. Rev. D* **4**, 2309 (1971).
  - [17] R. Carranza and C. C. Gerry, *J. Opt. Soc. Am. B* **29**, 2581 (2012).
  - [18] U. L. Andersen, T. Gehring, C. Marquardt, and G. Leuchs, *Physica Scripta* **91** (2015).
  - [19] G. Breitenbach, S. Schiller, and J. Mlynek, *Nature* **387**, 471 (1997).
  - [20] C. K. Hong and L. Mandel, *Phys. Rev. Lett.* **56**, 58 (1986).
  - [21] J. Krause, M. O. Scully, and H. Walther, *Phys. Rev. A* **36**, 4547 (1987).
  - [22] F. W. Cummings and A. K. Rajagopal, *Phys. Rev. A* **39**, 3414 (1989).
  - [23] B. T. H. Varcoe, S. Brattke, M. Weidinger, and H. Walther, *Nature* **403**, 743 (2000).
  - [24] Y. xi Liu, L. F. Wei, and F. Nori, *Europhys. Lett (EPL)* **67**, 941 (2004).
  - [25] E. Waks, E. Diamanti, and Y. Yamamoto, *New. J. Phys* **8**, 4 (2006).
  - [26] A. A. Houck, D. I. Schuster, J. M. Gambetta, J. A. Schreier, B. R. Johnson, J. M. Chow, L. Frunzio, J. Majer, M. H. Devoret, S. M. Girvin, and R. J. Schoelkopf, *Nature* **449**, 328 (2007).
  - [27] C. Monroe, D. M. Meekhof, B. E. King, S. R. Jefferts, W. M. Itano, D. J. Wineland, and P. Gould, *Phys. Rev. Lett.* **75**, 4011 (1995).



- [28] H. P. Yuen, *Phys. Rev. A* **13**, 2226 (1976).
- [29] M. Ashfaq Ahmad, S. Hamad Bukhari, S. Naeem Khan, Z. Ran, Q. Liao, and S. Liu, *Journal of Modern Optics* **58**, 890 (2011).
- [30] A. Biswas and G. S. Agarwal, *Phys. Rev. A* **75**, 032104 (2007).
- [31] G. S. Agarwal and K. Tara, *Phys. Rev. A* **43**, 492 (1991).
- [32] Y. Turek, A. Islam, and A. Abliz, *Eur. Phys. J. Plus* **138**, 72 (2023) (2021).
- [33] J. von Neumann, *Mathematical Foundations of Quantum Mechanics*, edited by N. A. Wheeler (Princeton University Press, Princeton, 2018).
- [34] A. Mari and J. Eisert, *Phys. Rev. Lett.* **103**, 213603 (2009).
- [35] D. W. C. Brooks, T. Botter, S. Schreppler, T. P. Purdy, N. Brahms, and D. M. Stamper-Kurn, *Nature* **488**, 476 (2012).
- [36] L.-A. Wu, H. J. Kimble, J. L. Hall, and H. Wu, *Phys. Rev. Lett.* **57**, 2520 (1986).
- [37] S. L. Braunstein and H. J. Kimble, *Phys. Rev. Lett.* **80**, 869 (1998).
- [38] Y. Yamamoto and H. A. Haus, *Rev. Mod. Phys.* **58**, 1001 (1986).
- [39] H. Yuen and J. Shapiro, *IEEE Transactions on Information Theory* **26**, 78 (1980).
- [40] R. Lo Franco, G. Compagno, A. Messina, and A. Napoli, *Phys. Rev. A* **72**, 053806 (2005).
- [41] R. Lo Franco, G. Compagno, A. Messina, and A. Napoli, *Phys. Rev. A* **76**, 011804 (2007).
- [42] S. L. Braunstein and H. J. Kimble, *Phys. Rev. A* **61**, 042302 (2000).
- [43] V. Petersen, L. B. Madsen, and K. Mølmer, *Phys. Rev. A* **72**, 053812 (2005).
- [44] J. Kempe, *Phys. Rev. A* **60**, 910 (1999).
- [45] G. Agarwal, *Quantum Optics* (Cambridge University Press, Cambridge, England, 2013).
- [46] Y. Turek, W. Maimaiti, Y. Shikano, C.-P. Sun, and M. Al-Amri, *Phys. Rev. A* **92**, 022109 (2015).
- [47] S. Pang and T. A. Brun, *Phys. Rev. Lett.* **115**, 120401 (2015).
- [48] Y. Turek, *Chinese Physics B* **29**, 090302 (2020).
- [49] C. Gerry and P. Knight, *Introductory Quantum Optics* (Cambridge University Press, Cambridge, England, 2004).
- [50] Z. Z. Xin, D. B. Wang, M. Hirayama, and K. Matsumoto, *Phys. Rev. A* **50**, 2865 (1994).
- [51] K. J. Blow, R. Loudon, S. J. D. Phoenix, and T. J. Shepherd, *Phys. Rev. A* **42**, 4102 (1990).